Competing interplay between Rashba and cubic-*k* Dresselhaus spin-orbit interactions in spin-Hall effect

R. S. Chang,[1] C. S. Chu,[1,2] and A. G. Mal'shukov[1,2,3]
[1]*Department of Electrophysics, National Chiao Tung University, Hsinchu 30010, Taiwan*
[2]*National Center for Theoretical Sciences, Physics Division, Hsinchu 30043, Taiwan*
[3]*Institute of Spectroscopy, Russian Academy of Science, 142190 Troitsk, Moscow oblast, Russia*
(Received 5 March 2009; revised manuscript received 20 April 2009; published 14 May 2009)

Focusing on the interplay between the Rashba and cubic-*k* Dresselhaus spin-orbit interactions (SOI), we calculate the spin accumulation S_z and the spin polarizations S_i^B at, respectively, the lateral edges and in the bulk of the two-dimensional electron gas. Their dependences on both the ratio between the Rashba and the Dresselhaus SOI coupling constants and the electron densities are studied systematically. Strong competition features in S_z are found. In the Dresselhaus-dominated regime S_z changes sign when the electron density is large enough. In the Rashba-dominated regime S_z is essentially suppressed. Most surprising is our finding that the Rashba-dominated regime occurs when $\alpha \approx 2\tilde{\beta}$, where α and $\tilde{\beta}$ are the Rashba and the effective linear-*k* Dresselhaus SOI coupling constants, respectively. For the spin polarizations S_i^B, the Rashba-dominated regime occurs when $\alpha \geq \tilde{\beta}$. Our results point out that decreasing $|\alpha|$ leads to the restoration of the spin accumulation S_z.

DOI: 10.1103/PhysRevB.79.195314 PACS number(s): 72.25.Dc, 71.70.Ej, 75.40.Gb, 85.75.−d

I. INTRODUCTION

Spin-orbit interaction (SOI) provides the key leverage for the recent strive for all electrical generations and manipulations of spin densities in semiconductors.[1–9] Intrinsic SOIs, such as the Rashba SOI (RSOI) (Refs. 3, 7, and 9–12) and the Dresselhaus SOIs (DSOIs),[6,13,14,23] are of particular interest. It is due to their tunability, gate tuning for the RSOI and either sample thickness or electron-density tuning for the DSOI, and to their physical origins, being independent of disorder that requires the presence of SOI impurities. Yet the ever present background scatterers do play a subtle role in the intrinsic spin-Hall effect.[15] In spin-Hall effect (SHE), an external electric field induces a transverse spin current and, in turn, an out-of-plane spin accumulation S_z at lateral edges.[1,5–9] For intrinsic SOIs, the background scatterers lead to a complete quenching of the edge spin accumulation S_z when the SOI depends only linearly on the electron momentum k,[15] but S_z maintains finite and dependent on the momentum relaxation time τ when the SOI has a cubic-*k* dependence.[14–17] Thus, separately considered, the RSOI does not contribute to edge spin accumulation S_z while the cubic-*k* DSOI does. For a more realistic situation, when the two SOIs coexist in a sample, RSOI could exert its effect on the edge spin accumulation S_z, but that would have to be mediated through the cubic-*k* DSOI. It is of great interest to see whether this effect would be reinforcing or competing for S_z.

Thus, in this work, we focus upon the interplay between the RSOI and the cubic-*k* DSOIs in their combined, or competing, effects on both the edge spin accumulation S_z and the bulk spin density S_i^B. Bulk spin density S_i^B, formed in an external electric field, is another important physical quantity of interest that is closely related to the intrinsic SOIs. The subscript i denotes the vector component of spin. The effect of the background scatterers on S_i^B is less subtle than that on S_z: S_i^B, remains finite for all intrinsic SOIs and depends on τ also.[3] Intuitively, up to leading order in the SOI coupling constant one might expect this S_i^B feature to arise from a SOI-effective magnetic field.[4] It turns out to be the case when there is only one dominated SOI and the SOI depends on k linearly. Take, for instance, a Rashba-type two-dimensional electron gas (2DEG) in the diffusive regime, the k-dependent effective magnetic field becomes $\langle \mathbf{h_k} \rangle = -\alpha \mathbf{z} \times \langle \mathbf{k} \rangle$ when $\langle \mathbf{k} \rangle$ is averaged over the electron distribution given by a shifted Fermi sphere $f(\epsilon, \mathbf{k}) = f_0(\epsilon, \mathbf{k}) - \frac{\tau e \hbar \mathbf{k} \cdot \mathbf{E}}{m^*} \delta(\epsilon_F - \epsilon)$, where α, f_0, and m^* are, respectively, the Rashba coupling constant, Fermi-Dirac distribution, and electron mass and for $e > 0$. With $\langle \mathbf{h_k} \rangle = \alpha \tau e / \hbar \hat{\mathbf{z}} \times \mathbf{E}$, the bulk spin density, in units of $\hbar$, is given by $\mathbf{S}^B = -N_0 \alpha \tau e / \hbar \hat{\mathbf{z}} \times \mathbf{E}$, which was first obtained by Edelstein.[3] In the above expression the density of states per spin is denoted by N_0. Beyond leading order or linear k dependence in the SOIs, or for the coexistence of different types of SOIs, the derivation of S_i^B becomes more involved. In this work, we calculate the S_i^B within a spin-diffusion equation approach and perform a systematic study on the competing interplay between the RSOI and the cubic-*k* SOIs.

Interplay between the RSOI and the linear-*k* DSOI in a sample has attracted much attention lately.[18–29] Earlier work studied the effect of $\alpha = \tilde{\beta}$, where $\tilde{\beta}$ is the effective linear-*k* DSOI coupling constant, on the magnetoconductivity.[18] More recent work on the same $\alpha = \tilde{\beta}$ regime pointed out that the spin becomes a good quantum number, independent of k, and has a long relaxation time.[19] The D'yakonov-Perel' (DP) mechanism[1] for spin relaxation is suppressed. This finding led to proposals for spintronic transistor that would manipulate polarized spin transport in the diffusive regime.[19,20] It was later shown, within the same $\alpha/\tilde{\beta} = 1$ regime, that the Fermi circles of opposite spins are connected by a wave vector $\mathbf{Q}$ that depends only on the SOI constant and the effective mass.[24] This leads to the persistent spin-helix state.[24] Since the ratio $\alpha/\tilde{\beta}$ is important for the development of spintronics, and the transport is anisotropic when both α and $\tilde{\beta}$ are

finite,[22,23,26–29] a number of experiments were designed to extract this ratio by the monitoring of the spin photocurrent.[22,26,27] Most of the studies dealt with the linear-k SOIs. One of the exceptions is a weak localization experiment that has extracted α, $\tilde{\beta}$, and also the cubic-k DSOI coupling constant from comparing the magnetoconductance data with a weak localization theory.[21] The delicate interplay between the RSOI and the cubic-k DSOI is yet to be explored and is much needed in either the spin transport, as is briefed above, or in the spin accumulations, as is related to SHE.

To study the interplay between the RSOI and the cubic-k DSOI in the diffusive regime, we extend our previous studies on the spin diffusive in a 2DEG strip to include both types of the SOI.[17] The diffusive regime has $l_e < L_{\rm so}$, where $L_{\rm so}$ and l_e are, respectively, the typical spin-relaxation length due to either the RSOI or the DSOI and the momentum-relaxation length. We study in detail the variations in S_z and S_i^B with respect to $\alpha/\tilde{\beta}$ and to the electron density. Our result shows Dresselhaus-dominated and Rashba-dominated regimes are determined primarily by the ratio $\alpha/\tilde{\beta}$. In the intermediate regime, intricate interplay between the RSOI and cubic-k DSOI is clearly shown as the electron density is varied. The edge spin accumulation S_z is essentially suppressed in the Rashba-dominated regime. Most surprisingly is our finding that the Rashba-dominated regime occurs when $\alpha \approx 2\tilde{\beta}$ for the edge spin accumulation S_z and when $\alpha = \tilde{\beta}$ for the bulk spin polarization S_i^B. Our result points to a possible way to restore the DSOI's contribution to the SHE, namely, to lower $|\alpha/\tilde{\beta}|$ to values well below unity. In Sec. II we present the spin-diffusion equation and the analytical solutions. In Sec. III we present our numerical results and discussions. Finally, in Sec. IV, we will present our conclusion.

II. THEORY

The system we consider is a 2DEG confined in an infinite strip with transverse boundaries at $y = \pm d/2$. The thickness of the strip $w \ll d$. An electric field $\mathbf{E}$ in the x direction induces the SHE. The phenomenon is described by a spin-diffusion equation[14,17] which has been derived from the Keldysch nonequilibrium Green's function method.[30] It has also been extended to the case of an in-plane magnetic field.[31] Detail of the derivation is not repeated here, but we will describe the physical meaning of the terms in the spin-diffusion equation. For our purpose here, the SOI magnetic field $\mathbf{h_k}$ includes both the RSOI and the cubic-k DSOI and is separated into linear-k and cubic-k terms $\mathbf{h_k} = \mathbf{h}_{\mathbf{k},1} + \mathbf{h}_{\mathbf{k},3}$. In a 2DEG, $\mathbf{h_k}$ lies on the two-dimensional plane after we average it with the lowest subband wave function over its thickness. Explicitly, we have

$$\mathbf{h}_{\mathbf{k},1} = \alpha(k_y, -k_x) + \beta\kappa^2(-k_x, k_y),$$

$$\mathbf{h}_{\mathbf{k},3} = \beta(k_x k_y^2, -k_y k_x^2). \tag{1}$$

Here, β is the DSOI coupling constant, $\kappa^2 = \langle k_z^2 \rangle$, and k_x and k_y are along, respectively, the [100] and [010] directions for a zinc-blende crystal.[32] It is convenient to define the effective linear-k DSOI coupling constant $\tilde{\beta} = \beta\kappa^2$. The SOI hamiltonian $\mathbf{H}_{\rm so} = \mathbf{h_k} \cdot \boldsymbol{\sigma}$, where $\boldsymbol{\sigma}$ is the Pauli-matrix vector.

Equation (1) provides us a simple way to get at the direction of the effective magnetic field $\mathbf{h_k}$ for a given electron distribution in the $\mathbf{k}$ space. This is important for an intuitive understanding of the spin-diffusion equation. From $\mathbf{h_k} = -\mathbf{h}_{-\mathbf{k}}$, the effective magnetic field is zero when the $\mathbf{k}$-space occupation is symmetric, as it is for the equilibrium case. If the deviation from equilibrium is a shifted distribution characterized by a wave vector $\mathbf{Q}$, then the effective magnetic field $\mathbf{h}^R$ due to RSOI will be along the direction of $\hat{\mathbf{Q}} \times \hat{\mathbf{z}}$. The DSOI case is less straight forward, but when $\mathbf{Q}$ is along either k_x or k_y, then $\mathbf{h}^D$ will be along or opposite to $\hat{\mathbf{Q}}$. Specifically, in the low electron-density ($k_F \ll \kappa$) regime $\mathbf{h}^D$ will be opposite (along) to $\mathbf{Q}$ when $\mathbf{Q}$ is along k_x (k_y). The direction of $\mathbf{h}^D$ will be reversed in the high-density ($k_F \gg \kappa$) regime. Here k_F is the Fermi wave vector.

The stationary spin-diffusion equations are given by

$$D\frac{\partial^2}{\partial y^2}S_z + \frac{R^{zxy}}{\hbar}\frac{\partial}{\partial y}S_x + \frac{R^{zyy}}{\hbar}\frac{\partial}{\partial y}S_y - \frac{\Gamma^{zz}}{\hbar^2}S_z = 0,$$

$$D\frac{\partial^2}{\partial y^2}S_y + \frac{R^{yzy}}{\hbar}\frac{\partial}{\partial y}S_z - \frac{\Gamma^{yy}}{\hbar^2}S_y - \frac{\Gamma^{yx}}{\hbar^2}S_x - \frac{C_y}{\hbar^2} = 0,$$

$$D\frac{\partial^2}{\partial y^2}S_x + \frac{R^{xzy}}{\hbar}\frac{\partial}{\partial y}S_z - \frac{\Gamma^{xx}}{\hbar^2}S_x - \frac{\Gamma^{xy}}{\hbar^2}S_y - \frac{C_x}{\hbar^2} = 0, \tag{2}$$

where diffusion constant $D = v_F^2\tau/2$, and S_i is the spin density in units of $\hbar$. Since $k_F l_e \gg 1$, charge neutrality is maintained by the condition of zero net charge density throughout.

The DP spin-relaxation rates $\Gamma^{il} = 4\tau\overline{h_k^2(\delta^{il} - n_k^i n_k^l)}$ for $i, l \in 1$, 2, and 3, for unit vector $\mathbf{n_k} = \mathbf{h_k}/h_k$. The overline denotes the angular average over the Fermi surface. Specifically, we have $\Gamma^{xx} = \Gamma^{yy} = \Gamma^{zz}/2 = 2\tau k_F^2(\alpha^2 + \tilde{\beta}^2 - \frac{1}{2}\tilde{\beta}^2\tilde{k}^2 + \frac{1}{8}\tilde{\beta}^2\tilde{k}^4)$ and $\Gamma^{xy} = \Gamma^{yx} = -\alpha\tau k_F^2\tilde{\beta}(4 - \tilde{k}^2)$ for $\tilde{k} = k_F/\kappa$. The diagonal components of the DP spin-relaxation rate receive independent contributions from the individual SOI. The off-diagonal DP components, however, involve both SOIs together, as they are proportional to $\alpha\tilde{\beta}$. Furthermore, $\tilde{k}$ serves as an agent that carries the cubic-k effects of the DSOI. For example, the term that has $\tilde{\beta}^2\tilde{k}^2$ is resulted from mixing the linear-k and the cubic-k effects of the DSOI, whereas the term that has $\tilde{\beta}^2\tilde{k}^4$ is due solely to the cubic-k effect of the DSOI, and in its second order.

Spin precession arising from spatial nonuniformity in spin densities is characterized by coefficients $R^{ilm} = 4\tau\Sigma_n \varepsilon^{iln}\overline{h_k^n v_F^m}$, where ε^{iln} is the Levi-Civita symbol. Specifically, the RSOI's contributions are $R^{yzy} = -R^{zyy} = \frac{2\pi k_F^2}{m^*}\alpha$, and the DSOI's contributions are $R^{zxy} = -R^{xzy} = \frac{2\pi k_F^2}{m^*}(\tilde{\beta} - \frac{1}{4}\tilde{\beta}\tilde{k}^2)$. As we will explore the interplay between the two SOIs by varying α while keeping $\tilde{\beta}$ fixed, it is more convenient to define the length scale $l_{\rm so} = 2D/R^{zxy}$ according to the strength of $\tilde{\beta}$ only. The coefficient R^{ilm}, if not zero, causes the precession of S_l, due to its

spatial variation along $\hat{m}$, to rotate into S_i. That R^{zyy}, for instance, receives sole contribution from RSOI can be understood from our aforementioned shifted electron-distribution picture. Taking that $S_y(q_y)$ is represented by a shifted distribution with $\hat{\mathbf{Q}}=-\hat{\mathbf{y}}$, the effective magnetic field $\mathbf{h}^{\mathbf{R}}$ due to RSOI will be along $\hat{\mathbf{Q}}\times\hat{\mathbf{z}}=-\hat{\mathbf{x}}$, leading to the precession of S_y about $\hat{x}$ clockwise. On the other hand, the effective magnetic field $\mathbf{h}^{\mathbf{D}}$ due to DSOI for this case will be along $-\hat{y}$, assuming low electron-density regime, and cannot lead to the precession of S_y. Similar argument can be applied to explain why R^{zxy}, for instance, receives contribution from DSOI only.

The effect of the driving electric field on the above spin diffusion enters through the coefficients C_i, for $i\in 1,2$. It is given by $C_i=\frac{1}{2}M_x^{i0}\partial D_0^0/\partial x$, where $M_x^{i0}=4\tau^2 h_k^3\frac{\partial n_k^i}{\partial k_x}$ incorporates the spin-charge coupling and $D_0^0=-2N_0eEx$ is a local equilibrium density.[17] The bulk spin densities can be solved directly from Eq. (2). We obtain $S_y^B=\frac{-C_x\Gamma^{yx}+C_y\Gamma^{xx}}{\Gamma^{xy}\Gamma^{yx}-\Gamma^{xx}\Gamma^{yy}}$, $S_x^B=\frac{C_x\Gamma^{yy}-C_y\Gamma^{xy}}{\Gamma^{xy}\Gamma^{yx}-\Gamma^{xx}\Gamma^{yy}}$, and $S_z^B=0$. The full expressions are given by

$$S_x^B=\left(\frac{\tau N_0 eE\tilde{\beta}}{2\hbar}\right)\times\frac{(8\alpha^4-16\alpha^2\tilde{\beta}^2+8\tilde{\beta}^4)+(2\alpha^4+8\alpha^2\tilde{\beta}^2-10\tilde{\beta}^4)\tilde{k}^2+(\alpha^2\tilde{\beta}^2+3\tilde{\beta}^4)\tilde{k}^4+\left(-\frac{3}{8}\alpha^2\tilde{\beta}^2+\frac{1}{8}\tilde{\beta}^4\right)\tilde{k}^6-\frac{5}{16}\tilde{\beta}^4\tilde{k}^8+\frac{3}{64}\tilde{\beta}^4\tilde{k}^{10}}{(-4\alpha^4+8\alpha^2\tilde{\beta}^2-4\tilde{\beta}^4)+(-4\alpha^2\tilde{\beta}^2+4\tilde{\beta}^4)\tilde{k}^2-2\tilde{\beta}^4\tilde{k}^4+\frac{1}{2}\tilde{\beta}^4\tilde{k}^6-\frac{1}{16}\tilde{\beta}^4\tilde{k}^8},$$

$$S_y^B=\left(\frac{\tau N_0 eE\alpha}{2\hbar}\right)\times\frac{(8\alpha^4-16\alpha^2\tilde{\beta}^2+8\tilde{\beta}^4)+(12\alpha^2\tilde{\beta}^2-12\tilde{\beta}^4)\tilde{k}^2+(\alpha^2\tilde{\beta}^2+3\tilde{\beta}^4)\tilde{k}^4-\frac{1}{4}\tilde{\beta}^4\tilde{k}^6+\frac{3}{16}\tilde{\beta}^4\tilde{k}^8}{(-4\alpha^4+8\alpha^2\tilde{\beta}^2-4\tilde{\beta}^4)+(-4\alpha^2\tilde{\beta}^2+4\tilde{\beta}^4)\tilde{k}^2-2\tilde{\beta}^4\tilde{k}^4+\frac{1}{2}\tilde{\beta}^4\tilde{k}^6-\frac{1}{16}\tilde{\beta}^4\tilde{k}^8}. \quad (3)$$

Equation (3) reduces to the pure RSOI result[3] when $\tilde{\beta}=0$, and to the pure cubic-k DSOI result[17] when $\alpha=0$. If the cubic-k term in the DSOI is dropped ($\tilde{k}=0$), Eq. (3) gives $\mathbf{S}_{\mathrm{LRD}}^B=-\frac{\tau N_0 eE}{\hbar}(\tilde{\beta},\alpha)$ so that it points to the third quadrant in the x-y plane. For $\alpha=\tilde{\beta}$, $\mathbf{S}_{\mathrm{LRD}}^B$ forms 45° with the $-x$ axis.

We solve the spin-diffusion equation for the spin density S_i across the semiconductor strip. The boundary condition we use is derived from requiring the local spin-current density I_y^i, which is expressed in terms of both S_i and its spatial derivative $\partial S_i/\partial y$, to be zero in its transverse flow I_y^i at the lateral edges.[17] This is appropriate for a hard-wall boundary.[33,34] Extended to include both SOIs, the spin-current density is given by

$$I_y^z=-2D\frac{\partial}{\partial y}S_z-R^{zyy}(S_y-S_y^B)-R^{zxy}(S_x-S_x^B)+I_{sH}\delta_{iz},$$

$$I_y^y=-2D\frac{\partial}{\partial y}S_y-R^{yzy}S_z,$$

$$I_y^x=-2D\frac{\partial}{\partial y}S_x-R^{xzy}S_z. \quad (4)$$

The spin-current density in Eq. (4) has contribution from spin diffusion, via the spatial gradients in S_i, spin precession, via the R^{ilm} coefficients, and the electric field, via the bulk spin-current density I_{sH}. It is given by

$$I_{sH}=-R^{zyy}S_y^b-R^{zxy}S_x^b+4\tau^2 eEN_0 v_F^y\left(\frac{\partial\mathbf{h}_\mathbf{k}}{\partial k_x}\times\mathbf{h}_\mathbf{k}\right)_z. \quad (5)$$

III. NUMERICAL RESULTS AND DISCUSSIONS

In this section, we present the edge spin accumulation S_z and the bulk spin polarizations $\mathbf{S}^B$ for a 2DEG semiconductor strip that consists of both the RSOI and the cubic-k DSOI. For definiteness, material parameters are chosen to be consistent with GaAs: effective mass $m^*=0.067m_0$, with m_0 the electron mass; *Dresselhaus* SOI $\beta=27.5$ eV Å^3,[3,32] and $\tilde{\beta}(\equiv\beta\kappa^2)=2.22$ eV m for quantum well thickness $w=300$ Å. The width of the strip is $d=30$ μm, and the mean free path $l_e=1$ μm. Typical value of l_{so} for $n=1\times10^{15}$ m^{-2}, or $\tilde{k}=0.76$, is $l_{\mathrm{so}}=2.20$ μm. The electrons occupy only the lowest subband in the quantum well. An electric field $E=25$ mV/μm is applied along x to set up the spin-Hall phenomenon.

Figure 1 presents the spatial profile of S_z across the semiconductor strip. Besides the well-known odd-parity feature of S_z in the transverse coordinate y, Figs. 1(a)–1(d) show, for the given physical parameter ranges, that the spin accumulation S_z is sensitive to the ratio $\alpha/\tilde{\beta}$. S_z has the largest magnitude in Fig. 1(a), where $\alpha/\tilde{\beta}=0$; it exhibits sign changes in Figs. 1(b) and 1(c), where $\alpha/\tilde{\beta}=0.5$ and 1, respectively; and it is essentially suppressed in Fig. 1(d), when $\alpha/\tilde{\beta}=2.0$. The fact that the RSOI dominates as early as $\alpha/\tilde{\beta}=2.0$ is surprising.

Dependence of S_z on the electron density, or $\tilde{k}$, is also shown in Fig. 1. For the case of pure Dresselhaus SOI, the edge spin accumulation S_z increases with $\tilde{k}$. This feature corroborates with the fact that the cubic-k SOI is the major contributor to S_z. On the other hand, S_z can change sign by either increasing the electron density, as is shown by the $\tilde{k}=1.20$ curve in Fig. 1(b), or by increasing the $\alpha/\tilde{\beta}$ ratio, as is

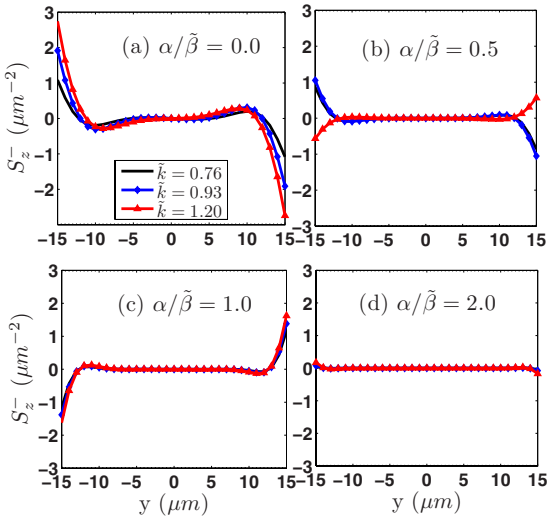

FIG. 1. (Color online) Spatial profile of spin density: S_z versus y. S_z in units of μm^{-2}, y in units of μm, and the width of the strip $d=30$ μm. $\tilde{k}=0.76$ (black solid line), 0.93 (blue diamond), and 1.20 (red triangle) correspond to electron density $n=1.0$, 1.5, and 2.5×10^{15} m^{-2}. The ratio $\alpha/\tilde{\beta}=0.0$, 0.5, 1.0, and 2.0 in (a)–(d), respectively.

shown by the curves in Fig. 1(c). This sign change in S_z is a manifestation of the competition between the RSOI and the cubic-k DSOI. That the RSOI joins forces with the cubic-k DSOI to compete with the pure cubic-k DSOI feature is an intriguing result we have found here. This is supported by Fig. 1(b), when the RSOI is of intermediate strength. The sign change in S_z occurs for the $\tilde{k}=1.20$ curve of which the cubic-k effect is the strongest. For larger RSOI, as in Fig. 1(c), the sign change occurs for all curves shown, including those of smaller $\tilde{k}$ values. All these characteristics, and the results in the following, have prompted us to categorize the spin accumulation into three regimes: the Dresselhaus-dominated regime, Fig. 1(a); the Rashba-dominated regime, Fig. 1(d); and the intermediate regime, Figs. 1(b) and 1(c). The ratio $\alpha/\tilde{\beta}$ is the key parameter that helps define these regimes. We note in passing that we have treated α and $\tilde{k}$ as though they were independent parameters whereas in practice they may be connected. It has been demonstrated experimentally, however, that the two parameters can be decoupled by a two gates technique.[35]

The dependence of the edge spin accumulation $S_z^- \equiv S_z(y=-d/2)$ at the sample edge on the regime parameter $\alpha/\tilde{\beta}$ is presented in Fig. 2. The first feature that we want to address about these curves is their even parity in $\alpha/\tilde{\beta}$. This confirms our expectation nicely because the symmetry of the system seems to demand a parity symmetry in S_z^- with respect to $\alpha/\tilde{\beta}$. However, the fact that $S_z^- \neq 0$ at $\alpha/\tilde{\beta}=0$ rules out the possibility for a S_z^- of odd parity, leaving us the even parity as the only choice. There are other features, which are equally important, in the general dependence of S_z^- on $\alpha/\tilde{\beta}$. Starting from a maximum at $\alpha/\tilde{\beta}=0$, S_z^- passes through a minimum of negative value and then diminishes to small values at $\alpha/\tilde{\beta}=2$. The minima occur within a region $0.5 < \alpha/\tilde{\beta} < 1$. These minima of S_z^- are resulted from the competition between the two SOIs. In contrast, the maximum of S_z^- is a pure DSOI feature. The maximum value of S_z^- increases with $\tilde{k}$ up to around $\tilde{k}=1.20$. Beyond this, the maximum value of S_z^- takes on a different course and decreases with increasing $\tilde{k}$ to negative values, as is indicated by the $\tilde{k}=1.51$ curve. Suppression on S_z^- is already quite significant when $\alpha/\tilde{\beta}>1.5$. On the other hand, taking both directions of S_z^- into account, $|\alpha/\tilde{\beta}|<1$ is the optimal region for the exhibition of spin accumulation.

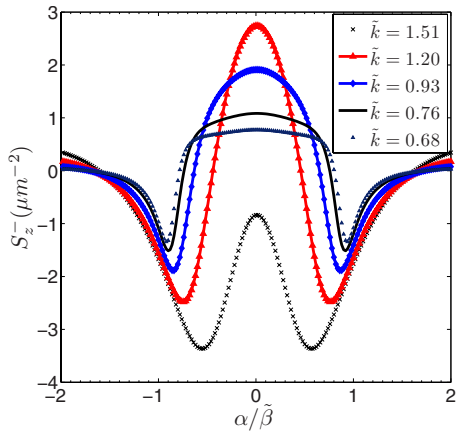

FIG. 2. (Color online) Edge spin accumulation S_z^- versus $\alpha/\tilde{\beta}$. $\tilde{k}=1.51$ (black cross), 1.20 (red triangle), 0.93 (blue diamond), 0.76 (black solid line), and 0.68 (black triangle) correspond to electron density $n=3.5$, 2.5, 1.5, 1.0, and 0.8×10^{15} m^{-2}, respectively. The curves show the symmetry $S_z^-(\alpha)=S_z^-(-\alpha)$.

Presented in Fig. 3 is the dependence of S_z^- on both $\tilde{k}$ and $\alpha/\tilde{\beta}$. It is meant to be a comprehensive presentation, with S_z^- versus $\tilde{k}$ curves plotted together for different values of $\alpha/\tilde{\beta}$ $(0\leq\alpha/\tilde{\beta}\leq2)$. The pure DSOI case is denoted by the circular dots and the $\alpha/\tilde{\beta}=1$ case is denoted by the open circles. The $\alpha/\tilde{\beta}=2$ case forms the boundary of the group of curves of increasing M, where the variation in S_z^- with $\tilde{k}$ is weak and the magnitudes small. It is convenient to describe the general features separately in two regions: the $0\leq\alpha/\tilde{\beta}\leq1$ and the $1\leq\alpha/\tilde{\beta}\leq2$ regions. In the former region the S_z^- increases with $\tilde{k}$ initially, following quite closely with the $\alpha/\tilde{\beta}=0$ curve, before it reaches its maximum. Beyond this point, S_z^- deviates from the $\alpha/\tilde{\beta}=0$ curve and decreases to pass through zero and into the negative value region. The increasing of $\alpha/\tilde{\beta}$ results in the negative shifting in the $\tilde{k}$ values of the zero of S_z^-. There is a tendency, as $\tilde{k}$ further increases, for the S_z^- to conform to the pure DSOI behavior, namely, that S_z^- increases its magnitude with $\tilde{k}$. This tendency, however, gradually fades out, for $\alpha/\tilde{\beta}>0.4$, and results in a much weaker dependence on $\tilde{k}$ when $\alpha/\tilde{\beta}\approx2$.

The domination of the pure DSOI in the small $\tilde{k}$ region is consistent with the understanding that the DSOI is the sole contributor to S_z^- there and the effect of RSOI needs to be

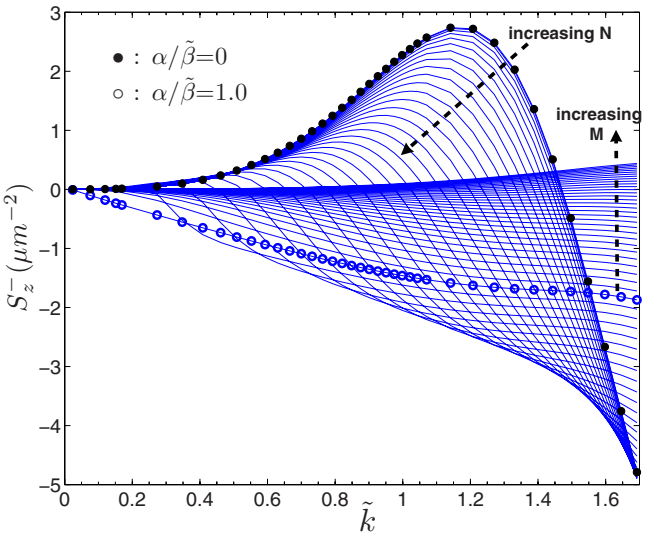

FIG. 3. (Color online) Spin densities S_z^- versus $\tilde{k}$. The case of pure Dresselhaus SOI ($\alpha/\tilde{\beta}=0$) is denoted by black circular dots. The case of $\alpha/\tilde{\beta}=1.0$ is indicated by blue open circles. Intermediate between them we have curves for $\alpha/\tilde{\beta}=N\times\Delta$, where $\Delta=\frac{1}{32}$. From $\alpha/\tilde{\beta}=1$ to $\alpha/\tilde{\beta}=2$ we have curves for $\alpha/\tilde{\beta}=1+M\times\Delta$. S_z^- is essentially suppressed when $\alpha\approx 2\tilde{\beta}$.

mediated by the cubic-k DSOI. The effects of RSOI emerge in larger $\tilde{k}$ values, where the location of the zero of S_z^- is negatively shifted with the increasing of $\alpha/\tilde{\beta}$. The zero of S_z^- can be understood with the vanishing of the effective magnetic field $\mathbf{h}=0$. Taking the $\alpha/\tilde{\beta}=0$ case as an example, $\langle\mathbf{h}^D\rangle=\langle[k_x(-\tilde{\beta}+\beta k_y^2),k_y(\tilde{\beta}-\beta k_x^2)]\rangle$. In a driving $\mathbf{E}$ field, the averages $\langle k_x\rangle=-\tau e/\hbar\mathbf{E}$ and $\langle k_y\rangle=0$ so that $\langle\mathbf{h}^D\rangle$ becomes zero if $\langle\tilde{\beta}-\beta k_y^2\rangle=0$. This condition is satisfied if $\tilde{k}=\sqrt{2}$, which is quite close to the value $\tilde{k}=1.47$ for the pure DSOI curve. We point out that the averages on $\mathbf{h}$ that enter into the contribution to the various processes considered in this work are much complicated than the one that we have just shown. But this nice correspondence in the $\tilde{k}$ values for the $\alpha/\tilde{\beta}=0$ case convinces us that the effective magnetic field concept is at work. This effect of α on the zero of S_z^- shows that the effect of RSOI is a competing one. Similar competing nature causes the suppression of the pure DSOI feature in the $\tilde{k}>1.2$ region. As is demonstrated by the $\alpha/\tilde{\beta}=1$ curve, the pure DSOI trend in this region no longer prevails but is largely suppressed. It is also of interest to see that S_z^- is negative in the entire shown values of $\tilde{k}$.

For the $1\leq\alpha/\tilde{\beta}\leq 2$ region, S_z^- decreases monotonically in its magnitude with the increasing of $\alpha/\tilde{\beta}$, while exhibiting a converging behavior as $\alpha/\tilde{\beta}$ increases. Except for a residual positive value for S_z^- in the large $\tilde{k}$ region when $\alpha/\tilde{\beta}=2$, the S_z^- is essentially suppressed.

In Figs. 4 and 5 we present both the bulk spin polarization $\mathbf{S}^B$ and its linear-k counterpart $\mathbf{S}^B_{\mathrm{LRD}}$ and their dependence on $\alpha/\tilde{\beta}$ and $\tilde{k}$. Relative magnitude between each vector pairs is shown, with the magnitude of $\mathbf{S}^B_{\mathrm{LRD}}$ chosen as unity. For a

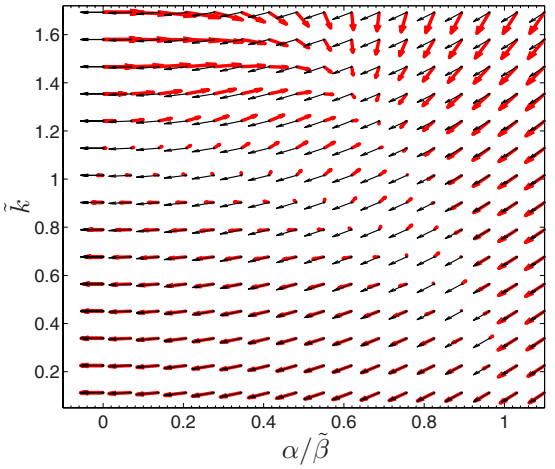

FIG. 4. (Color online) Bulk spin polarization $\mathbf{S}^B$ as a function of $\alpha/\tilde{\beta}$ (abscissa) and $\tilde{k}$ (ordinate), and for $0\leq\alpha/\tilde{\beta}\leq 1.2$. Directions of $\mathbf{S^B}$ are shown with x and y axes along the abscissa axis (pointing right) and the ordinate axis (pointing upward), respectively. $\mathbf{S}^B_{\mathrm{LRD}}$ (black arrows) denotes the linear-k SOIs, and $\mathbf{S}^B$ (red diffused arrows) denotes the full SOIs. The magnitudes of the vector pairs are normalized between themselves such that the magnitude of the bulk spin polarization is $|\mathbf{S}^B|/|\mathbf{S}^B_{\mathrm{LRD}}|$, and that of $\mathbf{S}^B_{\mathrm{LRD}}$ is unity.

fixed $\tilde{k}$, the two vector pairs become more aligned in both their directions and magnitudes when $\alpha/\tilde{\beta}$ increases. For a fixed $\alpha/\tilde{\beta}$ the general feature is that the vector pairs deviate more from each other as $\tilde{k}$ increases. This is consistent with the understanding that the deviation comes from the cubic k in the DSOI. There is an interesting intermediate region where the $\mathbf{S}^B\approx 0$. Starting from $\alpha/\tilde{\beta}=0$, the zero S^B is around $\tilde{k}\approx 1.1$. With the increasing of $\alpha/\tilde{\beta}$, the $\tilde{k}$ value for zero S^B decreases. This zero S^B feature ties up nicely with the zero S_z^- feature in Fig. 3 in that both of the $\tilde{k}$ values for the corresponding zeros decrease with the increasing of $\alpha/\tilde{\beta}$. Beyond the region $\alpha/\tilde{\beta}\geq 1$, the zero S^B feature subsides while the vector pairs align nicely with each other, both in

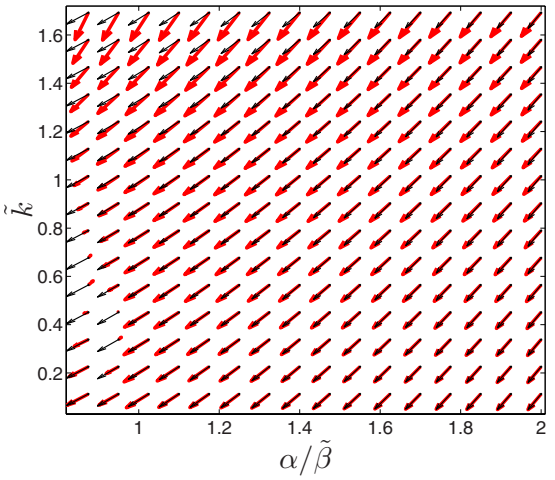

FIG. 5. (Color online) Bulk spin polarization $\mathbf{S}^B$ as a function of $\alpha/\tilde{\beta}$ and $\tilde{k}$, and for $0.9\leq\alpha/\tilde{\beta}\leq 2.0$.

direction and magnitude, unless for very large $\tilde{k}$. Thus the RSOI helps to make the linear-k SOI dominates in the formation of S^B for $\alpha/\tilde{\beta}>1$.

IV. CONCLUSION

In conclusion, we have studied systematically the competing interplay between the RSOI and the cubic-k DSOI in their contribution to the edge spin accumulation and the bulk spin polarization. There are three regimes, namely, the Dresselhaus-dominated regime ($|\alpha/\tilde{\beta}|<0.5$); the Rashba-dominated regime ($|\alpha/\tilde{\beta}|\approx 2$); and the intermediate regime ($0.5<|\alpha/\tilde{\beta}|\approx 1$). The optimal restoration of the spin accumulation occurs in the region $|\alpha/\tilde{\beta}|<1.0$. While the RSOI alone cannot give rise to spin accumulation, it can still exert its effect via the cubic-k DSOI, and thus provide the needed tunability for spin accumulations.

ACKNOWLEDGMENTS

This work was supported by Taiwan NSC (Contract No. 96-2112-M-009-0038-MY3), NCTS Taiwan, Russian RFBR (Contract No. 060216699), and a MOE-ATU grant.

[1] M. I. Dyakonov and V. I. Perel, Phys. Lett. **35A**, 459 (1971).
[2] A. A. Bakun, B. P. Zakharchenya, A. A. Rogachev, M. N. Tkachuk, and V. G. Fleisher, JETP Lett. **40**, 1293 (1984).
[3] V. M. Edelstein, Solid State Commun. **73**, 233 (1990).
[4] A. G. Aronov, Yu. B. Lyanda-Geller, and G. E. Pikus, Sov. Phys. JETP **73**, 537 (1991).
[5] J. E. Hirsch, Phys. Rev. Lett. **83**, 1834 (1999).
[6] S. Murakami, N. Nagaosa, and S. C. Zhang, Science **301**, 1348 (2003).
[7] J. Sinova, D. Culcer, Q. Niu, N. A. Sinitsyn, T. Jungwirth, and A. H. MacDonald, Phys. Rev. Lett. **92**, 126603 (2004).
[8] Y. K. Kato, R. C. Myers, A. C. Gossard, and D. D. Awschalom, Science **306**, 1910 (2004).
[9] J. Wunderlich, B. Kaestner, J. Sinova, and T. Jungwirth, Phys. Rev. Lett. **94**, 047204 (2005).
[10] E. I. Rashba, Sov. Phys. Solid State **2**, 1109 (1960); Yu. A. Bychkov and E. I. Rashba, JETP Lett. **39**, 78 (1984).
[11] H. A. Engel, B. I. Halperin, and E. I. Rashba, Phys. Rev. Lett. **95**, 166605 (2005).
[12] H. A. Engel, E. I. Rashba, and B. I. Halperin, Phys. Rev. Lett. **98**, 036602 (2007).
[13] G. Dresselhaus, Phys. Rev. **100**, 580 (1955).
[14] A. G. Mal'shukov and K. A. Chao, Phys. Rev. B **71**, 121308(R) (2005).
[15] J. I. Inoue, G. E. W. Bauer, and L. W. Molenkamp, Phys. Rev. B **70**, 041303(R) (2004); E. G. Mishchenko, A. V. Shytov, and B. I. Halperin, Phys. Rev. Lett. **93**, 226602 (2004); A. A. Burkov, A. S. Núñez, and A. H. MacDonald, Phys. Rev. B **70**, 155308 (2004); R. Raimondi and P. Schwab, *ibid.* **71**, 033311 (2005); O. V. Dimitrova, *ibid.* **71**, 245327 (2005).
[16] B. A. Bernevig and S. C. Zhang, Phys. Rev. Lett. **95**, 016801 (2005).
[17] A. G. Mal'shukov, L. Y. Wang, C. S. Chu, and K. A. Chao, Phys. Rev. Lett. **95**, 146601 (2005).
[18] F. G. Pikus and G. E. Pikus, Phys. Rev. B **51**, 16928 (1995).
[19] J. Schliemann, J. C. Egues, and D. Loss, Phys. Rev. Lett. **90**, 146801 (2003).
[20] X. Cartoixà, D. Z.-Y. Ting, and Y.-C. Chang, Appl. Phys. Lett. **83**, 1462 (2003).
[21] J. B. Miller, D. M. Zumbühl, C. M. Marcus, Y. B. Lyanda-Geller, D. Goldhaber-Gordon, K. Campman, and A. C. Gossard, Phys. Rev. Lett. **90**, 076807 (2003).
[22] S. D. Ganichev, V. V. Bel'kov, L. E. Golub, E. L. Ivchenko, P. Schneider, S. Giglberger, J. Eroms, J. De Boeck, G. Borghs, W. Wegscheider, D. Weiss, and W. Prettl, Phys. Rev. Lett. **92**, 256601 (2004).
[23] S. Q. Shen, Phys. Rev. B **70**, 081311(R) (2004).
[24] B. A. Bernevig, J. Orenstein, and S. C. Zhang, Phys. Rev. Lett. **97**, 236601 (2006).
[25] M. H. Liu, K. W. Chen, S. H. Chen, and C. R. Chang, Phys. Rev. B **74**, 235322 (2006).
[26] L. Meier, G. Salis, I. Shorubalko, E. Gini, S. Schön, and K. Ensslin, Nat. Phys. **3**, 650 (2007).
[27] S. Giglberger, L. E. Golub, V. V. Bel'kov, S. N. Danilov, D. Schuh, C. Gerl, F. Rohlfing, J. Stahl, W. Wegscheider, D. Weiss, W. Prettl, and S. D. Ganichev, Phys. Rev. B **75**, 035327 (2007).
[28] M. Scheid, M. Kohda, Y. Kunihashi, K. Richter, and J. Nitta, Phys. Rev. Lett. **101**, 266401 (2008).
[29] M. Wang, K. Chang, and K. S. Chan, Appl. Phys. Lett. **94**, 052108 (2009).
[30] A. A. Abrikosov, L. P. Gorkov, and I. E. Dzyaloshinskii, *Method of Quantum Field Theory in Statistical Physics* (Dover, New York, 1975).
[31] L. Y. Wang, C. S. Chu, and A. G. Mal'shukov, Phys. Rev. B **78**, 155302 (2008).
[32] R. Winkler, *Spin-Orbit Coupling Effects in Two-Dimensional Electron and Hole Systems*, (Springer-Verlag, Berlin, 2003).
[33] O. Bleibaum, Phys. Rev. B **74**, 113309 (2006).
[34] Y. Tserkovnyak, B. I. Halperin, A. A. Kovalev, and A. Brataas, Phys. Rev. B **76**, 085319 (2007).
[35] D. Grundler, Phys. Rev. Lett. **84**, 6074 (2000).